Cellular Microbiology (2005) **7**(12), 1763–1770 doi:10.1111/j.1462-5822.2005.00593.x

# Surface ultrastructure of SARS coronavirus revealed by atomic force microscopy

**Shiming Lin,[1,2]* Chih-Kung Lee,[2] Shih-Yuan Lee,[3] Chuan-Liang Kao,[4] Chii-Wann Lin,[5] An-Bang Wang,[2] Su-Ming Hsu[6] and Long-Sun Huang[2]**

[1]*Center for Optoelectronic Biomedicine, National Taiwan University, Taipei, Taiwan.*

[2]*Institute of Applied Mechanics, National Taiwan University, Taipei, Taiwan.*

[3]*Department of Chemistry, Tamkang University, Taipei, Taiwan.*

[4]*Department of Medical Technology, National Taiwan University, Taipei, Taiwan.*

[5]*Institute of Biomedical Engineering, National Taiwan University, Taipei, Taiwan.*

[6]*Department of Pathology, National Taiwan University, Taipei, Taiwan.*

## Summary

**Atomic force microscopy has been used to probe the surface nanostructures of severe acute respiratory syndrome coronavirus (SARS-CoV). Single crown-like virion was directly visualized and quantitative measurements of the dimensions for the structural proteins were provided. A corona of large, distinctive spikes in the envelope was measured after treatment with hydroxyoctanoic acid. High-resolution images revealed that the surface of each single SARS-CoV was surrounded with at least 15 spherical spikes having a diameter of 7.29 ± 0.73 nm, which is in close agreement with that of S glycoproteins earlier predicted through the genomes of SARS-CoV. This study represents the first direct characterization of the surface ultrastructures of SARS-CoV particles at the nanometre scale and offers new prospects for mapping viral surface properties.**

## Introduction

A novel coronavirus has been identified as the probable cause of the newly recognized severe acute respiratory syndrome (SARS) (Ksiazek *et al*., 2003; Drosten *et al*., 2003; Peiris *et al*., 2003). The sequences of the complete genomes of two isolates of the SARS coronavirus (SARS-CoV) have been reported (Rota *et al*., 2003; Marra *et al*., 2003). Five major open reading frames (ORFs) were determined through sequence similarity to known coronavirus proteins. This approach identify two replicases 1a and 1b that undergo cotranslational proteolytic processing and four structural proteins the spike (S), envelope (E), membrane (M) glycoproteins and the nucleocapsid (N) protein (Holmes and Enjuanes, 2003). Understanding pathogenesis of SARS requires knowledge of the structure and physicochemical properties of the SARS-CoV surface at supramolecular scale. The ultrastructure of SARS-CoV virions has been characterized by thin-section electron microscopy (Ksiazek *et al*., 2003); however, direct information on the native viral surface was inaccessible.

The atomic force microscopy (AFM) (Binning and Quate, 1986), one of the scanning probe microscopy (Binning *et al*., 1982), has proved useful to investigate the topography of viral surfaces (Kuznetsov *et al*., 2002; 2004; 2005; Malkin *et al*., 2003; Nettikadan *et al*., 2003, Hughes *et al*., 2004; Negishi *et al*., 2004), because AFM images can reveal structural details with unprecedented resolution. While optical microscopes are limited by diffraction ($\lambda/2$), AFM can achieve molecular and even atomic resolution for many materials (Butt *et al*., 1993; Miura and Shukuya, 1993; Liu and Salmeron, 1994; Xu *et al*., 1998). In addition, three-dimensional information can be extracted directly from AFM topographic and phase images. These advantages force us to apply the AFM to the field of SARS-related virology. Here, we used AFM to determine the surface ultra structure of each single SARS-CoV virion and observe the surface characteristics and their topography and phase changes after treatments with hydroxyoctanoic acid or protease. This study provides a new approach to the measurements of components of SARS-CoV virions for future application in SARS proteomics.

## Results and discussion

### *Native SARS-CoV*

Figure 1 shows the AFM height images of the native SARS-CoV virions in the culture medium. In Fig. 1A, the surface was uniformly covered with a number of spherical

Received 12 April, 2005; revised 19 May, 2005; accepted 12 June, 2005. *For correspondence. E-mail sml@ntumc.org; Tel. (+886) 2 23123456 ext. 8458; Fax (+886) 2 23949125.

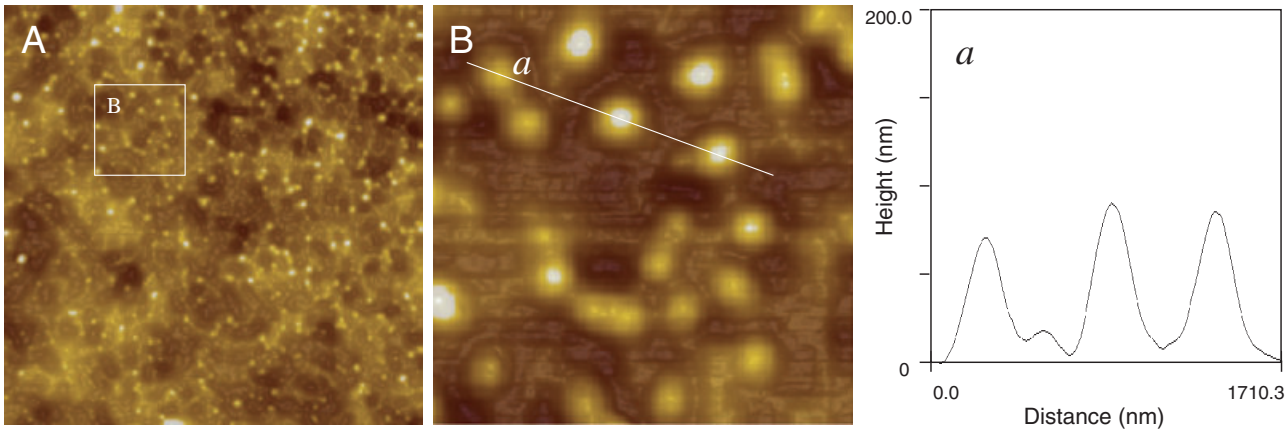


**Fig. 1.** Topographic AFM images of the native SARS-CoV particle on mica. The scanning areas are $10 \times 10$ μm$^2$ and $2 \times 2$ μm$^2$ for the low- (A) and high-resolution (B) images respectively. An image acquired by zooming into the boxed areas is displayed in B. The high-resolution image and corresponding cursor profile (*a*) clearly reveal the presence of SARS-CoV particles.

particles in the medium environment. An image acquired by zooming into the boxed area is displayed in Fig. 1B. The higher-resolution image shows that many individual spherical protrusions exist on the surface and the corresponding cursor profile (Fig. 1*a*) clearly reveals the presence of SARS-CoV particles and each single particle is readily distinguishable. The corresponding cursor profile provides quantitative measurements of the heights for the SARS-CoV particles on the surface. The profile displays that the measured heights of SARS-CoV particles are 71.7, 90.9 and 84.8 nm respectively. Over 30 single spherical particles were then examined, the surface traces are reproducible although some variations exist in the height of surface protrusions. The root mean square (RMS) value of heights of SARS-CoV particles calculated was approximately $81.2 \pm 10.6$ nm. After average height for each viral particle are calculated, it is found that the RMS value of height ($81.2 \pm 10.6$ nm) corresponds with that (80–110 nm in diameter) obtained from a thin-section electron microscopy (Ksiazek *et al*., 2003).

### *Crown-like SARS-CoV virions*

In previous study, a typical SARS-associated coronavirus has been found by the use of negative-stain electron microscopy which shows a stain-penetrated coronavirus particle with club-shaped surface projections surrounding the periphery of the particle (Ksiazek *et al*., 2003). To further investigate the surface ultrastructure of a single SARS-CoV virion by AFM, we treated SARS-CoV samples with the surface-modifying chemical, hydroxyoctanoic acid (Fig. 2). AFM images (scanning area $10 \times 10$ μm$^2$) of entire SARS-CoV after treatment are displayed in Fig. 2A (height image) and 2A′ (phase image) respectively. Higher-resolution height (Fig. 2B and C) and phase (Fig. 2B′ and C′) images (scanning area $2 \times 2$ μm$^2$) were obtained by zooming into the boxed areas displayed in Fig. 2A and A′ respectively. These higher-resolution images clearly reveal the presence of crown-like SARS-CoV virions and that each single virion with a partially intact or completely disrupted appearance is readily distinguishable. Each surface virion displayed in Fig. 2A was then profiled and their dimensions measured. It was found that, over 60 single particles were examined, the length, width and height of treated virions vary in a broad interval of 336–473 nm, 277–353 nm and 3.62–39.83 nm respectively.

Moreover, the phase images obtained were used to observe the surface characteristics. The phase images are useful for compositional mapping of surfaces with different stiffness of the constituting substances (Magonov *et al*., 1997). It allows us to identify immediately hard and soft material, the bright parts of the AFM image corresponding to hard material (e.g. yellow is stiffer than brown). As shown in Fig. 2B′, the phase image indicate the presence of some material (yellow, arrowheads in Fig. 2B′) surround the virus that was of a different composition than either the virion itself (brown) or the mica substrate (white). This may represent the chemicals (hydroxyoctanoic acid) interacted with the virions. In addition, as shown in Fig. 2C′, many spheres (brown, arrowheads in Fig. 2C′) were liberated and dispersed near the virion itself. This might be attributed to the breakdown of viral envelope caused by hydroxyoctanoic acid. Hydroxyoctanoic acid is speculated to have unusual effects on the surface chemistry of viral envelope. Upon exposure to hydroxyoctanoic acid, the viral surface of SARS-CoV became more heterogeneous (Fig. 2) than the native virus (Fig. 1).

To investigate the surface ultrastructure of a single SARS-CoV virion, over 60 SARS-CoV virions displayed in

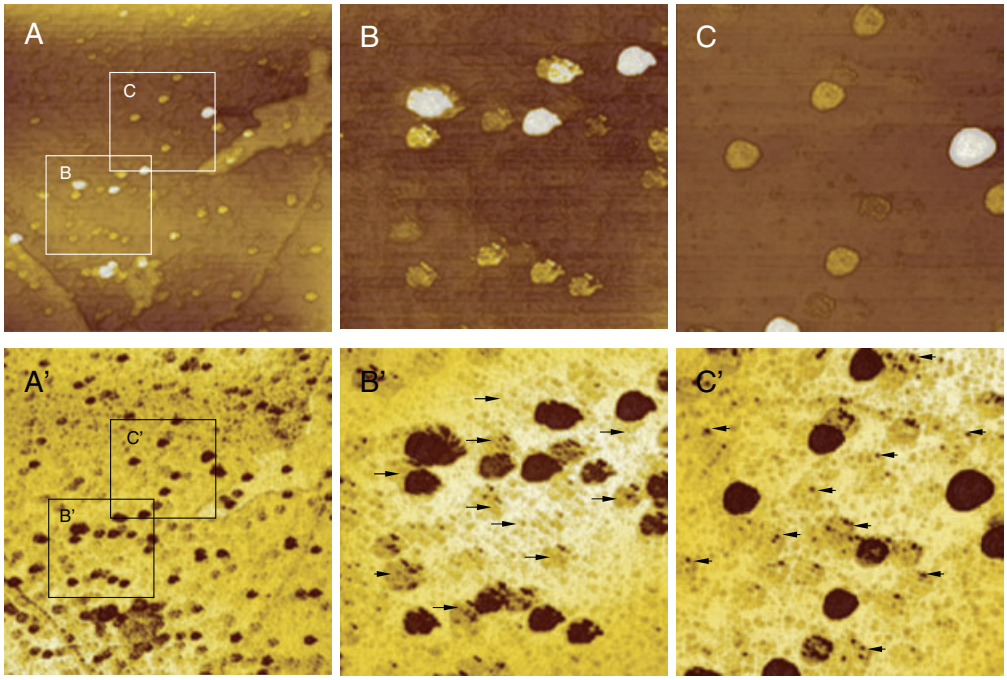


**Fig. 2.** AFM images of the SARS-CoV treated with hydroxyoctanoic acid. Height image (top row) and phase image (bottom row). Images of entire viruses are shown in left column (total scanning area $10 \times 10\ \mu m^2$). Images acquired by zooming into the boxed are displayed in the second and third columns (total scanning area $2 \times 2\ \mu m^2$) respectively. A new tip was used for the images in the third columns.

Fig. 2A were examined and their higher-resolution images (scanning area $500 \times 500\ nm^2$) obtained, and some images were shown in Fig. 3B–E for further observation and measurements. Native SARS-CoV virions in the environment of distilled water were completely not damaged and serve as a control (Fig. 3A). When viruses were exposed to hydroxyoctanoic acid, the viral morphology was affected. As shown in Fig. 3B–E, SARS-CoV treated with hydroxyoctanoic acid displayed heterogeneous surface features. The native virion was broken down and a corona of large, distinctive protrusions surrounding the envelope are readily observed in Fig. 3B. The appearance of pits as shown in Fig. 3C–E indicates the release of viral components, predominately structural proteins such as spike (S) protein, membrane (M) proteins, small envelope (E) proteins or nucleocapsid (N) proteins, or non-structural proteins (such as replicase 1a and 1b) (Ksiazek *et al.*, 2003; Rota *et al.*, 2003; Marra *et al.*, 2003; Holmes and Enjuanes, 2003). The new structure after treatment is not as tight as that of the native virion, which leads to liberation of the viral content (Fig. 3B–E). After treatment, intermolecular interactions among structural proteins (S, M or E proteins) within the envelope are weakened. Desorption of structural proteins occurs from the boundaries of the membrane patches, gradually leading to the release of some structural proteins. In addition, although the whole virions in some images (Fig. 3B–E) appeared disrupted to some extent, some particles which initially surround the periphery are still visible in AFM images, as indicated by the cursor profiles (Fig. 3*b–e*).

Moreover, hydroxyoctanoic acid caused a substantial reduction in the surface height and irregularity in the viral surfaces. The particles indicated by the cursor profiles (Fig. 3*b–e*) are probably larger structural proteins surrounding the viral periphery, such as spike proteins (*vide infra*). These regular structures are unlikely to be artifacts of either tip shape or immobilization procedure because they have been observed on at least 200 SARS-CoV virions which had been scanned in this work. The corresponding cursor profiles (Fig. 3*b–e*) provide quantitative measurements of the dimensions for the surface nanostructures. The profiles displayed in Fig. 3*b–e* shows that the maximum height of particles measured are approximately 15.25, 9.78, 7.72, 7.19 nm respectively. As shown in Fig. 3B and C, each spherical protrusion on the cursor *b* or *c* was surrounded by other components in the envelope, while the spherical protrusion on cursor *d* and *e* in Fig. 3D and E, respectively, may be nearly regarded as an individual particle for further measurement. Over 30 such particles as displayed on the cursor *d* and *e* were examined, and although some variations exist in the exact height of such particles, the surface traces are reproducible. The calculated RMS value of heights of particles is $7.29 \pm 0.73$ nm.

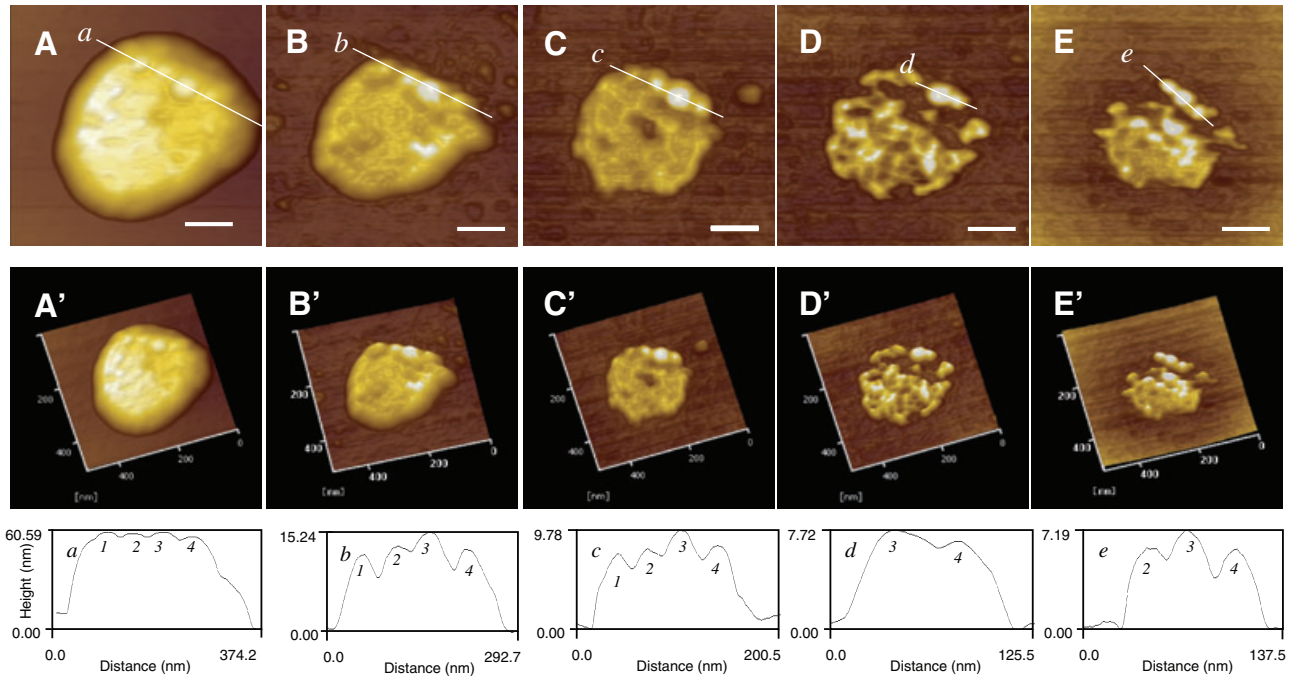


**Fig. 3.** Topographic AFM images of different single SARS-CoV virions before (the first column) and after (the second to fifth column) treatment with hydroxyoctanoic acid. Images acquired by zooming into the boxed areas in Fig. 2A are displayed in the B–E (two-dimensional) and B′–E′ (three-dimensional). Scale bar = 100 nm for each image in the first row. The corresponding cursor profiles (the third row) provide quantitative measurements of the dimensions for spike proteins.

*Chemical composition of spherical protrusions*

In order to get more information as to the chemical composition of these spherical protrusions in the envelope we scanned the area containing the SARS-CoV virions (in paired fashion) before and 15 min after treatment with the proteolytic enzyme, protease. As illustrated in Fig. 4 the images became blurred and the surface crown-like structures in the envelope considerably decreased approximately 70% in height over 15 min of protease treatment. This indicates that imaged spherical particles on the surface have been hydrolysed by protease action. This observation also shows that these spherical particles on virial surface are mainly composed of material which contain protein molecules.

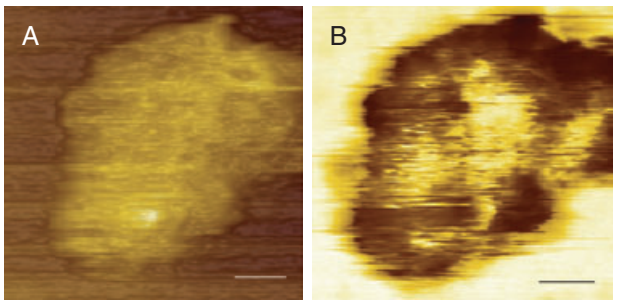


**Fig. 4.** AFM images of a SARS-CoV particle after treatment with protease. Height image and phase image of an individual virion is shown in A and B respectively. Scale bar = 50 nm for A and B.

*Spike proteins*

In previous studies the SARS-CoV genome was reported to contain six major ORFs through sequence similarity that encode two replicase polyproteins; and four structural proteins, the spike (S) protein, the small envelope (E) protein, the membrane (M) glycoprotein, and the nucleocapsid (N) protein (Rota *et al*., 2003; Marra *et al*., 2003). The numbers of amino acids of six coronavirus proteins identified are 4382, 2628, 1255, 76, 221 and 422, respectively (Marra *et al*., 2003), and thus the molecular weights of proteins predicted are approximately 526, 315, 151, 9, 27, and 51 kDa respectively. To investigate whether the spherical particles observed above are spike (S) proteins or other proteins in the viral envelope, immunoglobulin G (IgG) molecules (mol. wt. ≒ 150 kDa) which have the same molecular weight with the spike protein (approximately 151 kDa) were prepared and scanned for AFM imaging under the same conditions with SARS-CoV sample. Multiple cross-sections of the individual IgG images by AFM were made and mean diameter and height of each single molecule were measured. After average height for each IgG molecule is calculated, it was found that the RMS value of heights for IgG molecules is approx-

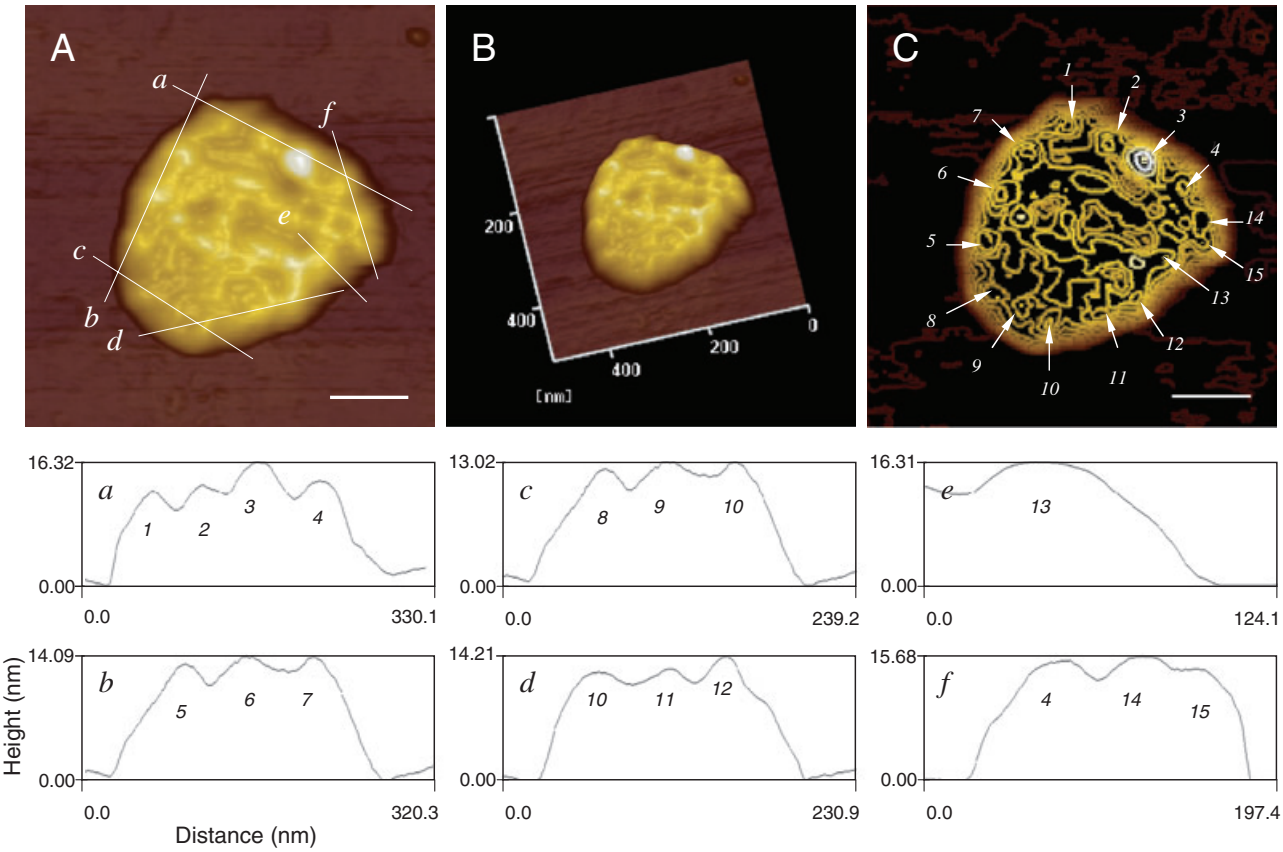


**Fig. 5.** (A) Two- and (B) three-dimensional AFM images and contour map (C) of a single SARS-CoV virion. Scale bar = 100 nm in A and C. The corresponding cursor profiles (middle and bottom row) provide quantitative measurements of the dimensions for the spike proteins (*1–15*) displayed in C.

imately 7.13 ± 0.13 nm (data not shown). This value is about consistent with the value (7.29 ± 0.73 nm) obtained for spherical particles (Fig. 3) surrounding on the surface of SARS-CoV. Thus, the spherical particles visible on the viral surface are speculated to be possibly spike (S) proteins because of their size, 7.29 ± 0.73 nm.

For those SARS-CoV virions that maintain their crown-shaped morphology, the high-resolution images (500 × 500 μm) shown in Fig. 5 reveal that a corona of large, distinctive spikes surrounding the envelope of SARS-CoV. These spikes in the envelope makes possible the identification of coronaviruses by AFM. Figure 5 shows the two- (Fig. 5A) and three-dimensional (Fig. 5B) AFM images and their contour map (Fig. 5C) of a single SARS-CoV virion. The corresponding cursor profiles (Fig. 5*a–f*) reveal couples of bumps and dents formed by the spikes proteins on the surface and also provide quantitative measurements of the dimensions for these spike proteins. It was found that from the contour map (Fig. 5C) 15 spike proteins (arrowheads) surround the envelope of a single SARS-CoV virion. It is thus speculated that at least 15 spike proteins form the whole corona of a single SARS-CoV virion. In addition, as the virion displayed in Fig. 5A does not represents an intact one, the thickness of its corona surrounding the periphery ranges approximately from 13 to 17 nm (Fig. 5*a–f*), which basically corresponds to the dimension (20- to 30-nm) of the corona of SARS-CoV obtained previously from electron microscopic study (Ksiazek *et al.*, 2003).

### *Small spherical particles released*

This work has also created a way to break down a new infectious agent, SARS-CoV, into small components. As shown in Fig. 6, after the intact virion was break down by chemical treatment, a number of small spherical particles (also see Fig. 2C′, arrowheads) were released and readily observed from the height (Fig. 6A) and phase (Fig. 6B) image. The phase image provides a measure of sample heterogeneity and also indicates that the small spherical particles (arrowheads) come from the SARS-CoV virion itself (Fig. 6B). The cursor profiles displayed in Fig 6*a* and *b* can provide quantitative measurement of the dimension for each small spherical particle observed in Fig. 6A.

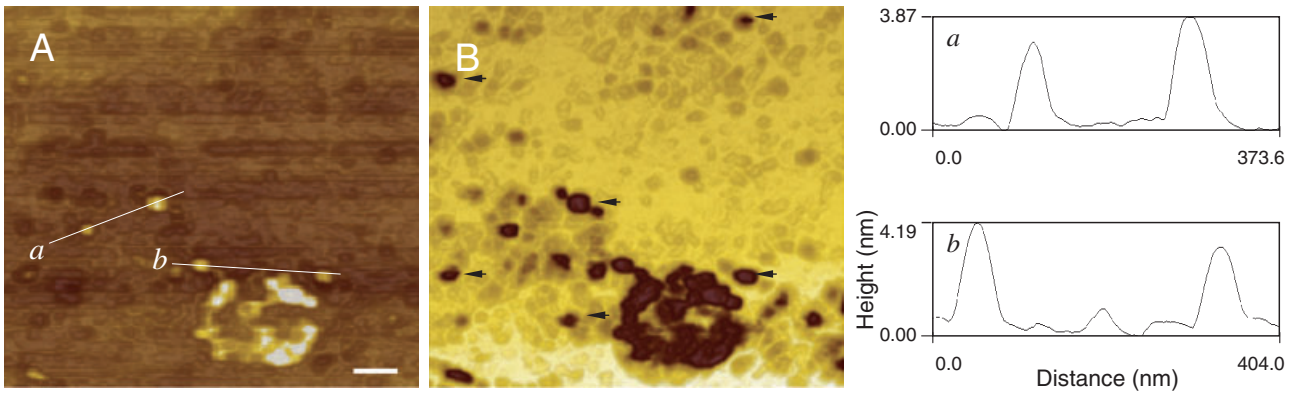


**Fig. 6.** Images acquired by zooming into the boxed areas in Fig. 2C are displayed in A (height image) and B (phase image). Scale bar = 200 nm. In the height image (A) a section line is placed through two small spherical particles. The resulting profiles (*a* and *b*) are shown in the right panel. The corresponding cursor profiles (*a* and *b*) provide quantitative measurements of the dimensions for the particles released from virion itself.

Over 30 various small spherical particles liberated were then examined, the heights of small spherical particles ranges from 2.83 to 4.57 nm. The structural proteins of SARS-CoV have been reported to include spike (S) protein (mol. wt. ≒ 151 kDa), membrane (M) protein (mol. wt. ≒ 27 kDa), small envelope (E) protein (mol. wt. ≒ 9 kDa) and nucleocapsid (N) protein (mol. wt. ≒ 51 kDa) (Marra *et al.*, 2003). Although SARS-CoV also encode a number of non-structural proteins that are of unknown function and located between S, and E, between M and N, or downstream of N, molecular weights of these non-structural proteins are predicted to be less than 32 kDa. (Rota *et al.*, 2003; Marra *et al.*, 2003). Thus, various sizes of small spherical particles (2.83–4.57 nm) released when SARS-CoV broke down represents the different types of proteins of SARS-CoV reported previously. Therefore, the study reported here provides an approach to measurement of some components of a single SARS-CoV virion for future application in SARS proteomics-related studies.

## Conclusions

We have shown that AFM is a useful technique in providing structural information for individual SARS-CoV virions. In addition, three-dimensional information on components in the envelope can be extracted from the topographic images. However, it should be noted that it is not possible to be absolutely definite in attributing topographical and phase features in AFM images to virions or viral debris. Whilst removing/avoiding impurities in sample preparation reduces the possibility of imaging third-party debris other methods are necessary to confirm the identification. Further work will concentrate on the use of antibody-nanogold conjugates for the identification of SARS-CoV virion particles.

In this work, we also revealed for the first time the surface image of individual SARS-CoV virions before and after treatment. Quantitative measurements of the dimensions for the spike (S) proteins in the envelope have been provided. The physical measurements of the S proteins in the SARS-associated coronavirus may suggest how S proteins affect the pathogenesis of SARS. We have also created a way to break down the SARS-CoV into small components. Then, people can quickly isolate and test the components to find out which one stimulates the best immune response for the future development of vaccines or new drugs for SARS.

## Experimental procedures

### *Severe acute respiratory syndrome coronavirus preparation*

Severe acute respiratory syndrome coronavirus (TW-1) (GenBank Accession no. AY29145) used in this study was originally isolated from the throat swab specimens of one patient in Taiwan. Throat swab specimens were inoculated into Vero E6 cells, cultured, and monitored (Hsueh *et al.*, 2003; Yeh *et al.*, 2004). Once the virus-induced cytopathic effects appeared, the culture cell supernatant containing viruses was harvested and impurities in sample preparation were removed as described (Hsueh *et al.*, 2003; Yeh *et al.*, 2004). All division into aliquots, pipetting, culture, treatments, and attachment attempts were performed in laminar-flow safety cabinets in a biosafety level 3 laboratory; after these steps, the sample preparations were removed to biosafety level 2 laboratory for completion of the AFM imaging.

### *Attachment of SARS-CoV to mica*

For AFM studies, SARS-CoV sample was attached through electrostatic interactions by placing in contact with a freshly cleaved mica that had been coated with poly L-lysine hydrobromide, a positively charged compound. After cleaning the mica with methanol and Milli-Q water, a drop of 0.01% (wt/vol) poly L-lysine hydrobromide solution was applied and incubated for 30 min. The mica surface was then washed with Milli-Q water before introduc-

tion of the SARS-CoV specimens. The specimen was applied onto the poly L-lysine-treated mica for 5 min at room temperature, followed by washing with distilled water (50 μl, three times) and drying in air prior to the AFM experiments.

### *Chemical treatment with hydroxyoctanoic acid*

The mica substrate adsorbed with SARS-CoV virions was washed with Milli-Q water before introduction of the chemical, hydroxyoctanoic acid. A 10 μl portion of the above chemical (0.1 mg $ml^{-1}$) in 20 mM PBS buffer, pH 7.2, was added to the mica substrate, followed by incubation for 5–10 min, removing of the residual chemical solution, and drying in air prior to the AFM experiments.

### *Protease treatment*

Protease from *Streptomyces griseus* (P5147, Sigma, USA) was dissolved in 10 mM sodium acetate buffer with 5 mM calcium acetate, pH 7.5 at a concentration of 50 μg $ml^{-1}$. A 10 μl portion of the above protease solution (20 units $ml^{-1}$) was added to the mica substrate immobilized with SARS-CoV virions, followed by washing with Milli-Q water three times and air-drying prior to the AFM experiments.

### *Atomic force microscopy experiments*

Atomic force microscopy experiments in tapping mode of operation were carried out using a multimode scanning probe microscope (SPI300 HV, Seiko Instruments, Chiba, Japan) in combination with a light microscope (Mitotoyo, Japan). AFM Tips were 200 μm long and had a typical resonant frequency of 140 kHz (Nanosensor, Wetzlar-Blankenfeld, Germany). Calibration of the AFM cantilever tip were carried out using a standard diffraction grating (Seiko Instruments, Chiba, Japan). Light tapping was used, which involved maintaining a high amplitude reference relative to the free amplitude of the cantilever. Typically, we began by scanning a 20 μm × 20 μm area that would contain hundreds of SARS-CoV virions. Gradually, the image size was reduced to isolate individual virion (500 nm × 500 nm). SARS-CoV specimen were scanned in both directions several times before capturing an image, to help ensure that tip artifacts, such as hysteresis, were not altering the images. Over 200 high-quality images were captured for each SARS-CoV virion, and a number of images were selected from these. Tips were replaced when there was any indication of artifacts present in the images. After images were collected, an offline section analysis was performed on each image in order to gain information on viral topography. When a line was drawn across the image, the topography of the sample as a function of distance was displayed. These height traces were performed to provide more information on how each treatment affected the surface topography. Roughness analyses were also performed on some samples, conducted according to the manufacturer's software program (SPI 3800N). The RMS average of the surface roughness value was calculated as the standard deviation of all the height values within the given area.

Phase images were captured simultaneously with height (topographic) images. In phase imaging, the phase shift of the oscillating cantilever is measured as a function of tip position on the surface. Height images reveal surface topography and are more accurate in detailing the height of features on the surface. Phase images have proved to yield better resolution in detailing the lateral dimensional data of surface features (Kopp-Marsaudon *et al*., 2000) but as the different factors that cause phase shift cannot be separated, interpretation of phase images can be much more difficult. Phase imaging is useful as a complement to topographic imaging for providing information on SARS-CoV sample heterogeneity.

## Acknowledgements

This work was supported in part by MEA 92-EC-17-A-05-S1-0017, NSC Grant 92-2320-B-002-123 and NSC Grant 93-2323-B-002-013.

## References

Binning, G., and Quate, C.F. (1986) Atomic force microscope. *Phys Rev Lett* **56:** 930–933.

Binning, G., Rohrer, G.H., Gerber, C.H., and Weibel, E. (1982) Surface studies by scanning tunneling microscopy. *Phys Rev Lett* **49:** 57–61.

Butt, H.J., Seifert, K., and Bamberg, E. (1993) Imaging molecular defects in alkanethiol monolayers with an atomic force microscope. *J Phys Chem* **97:** 7316–7320.

Drosten, C., Gunther, S., Preiser, W., Werf, S., Brodt, H.R., Becker, S., *et al.* (2003) Identification of a novel coronavirus in patients with severe acute respiratory syndrome. *N Engl J Med* **348:** 1967–1976.

Holmes, K.V., and Enjuanes, L. (2003) The SARS coronavirus: a postgenomic era. *Science* **300:** 1377–1378.

Hsueh, P.-R., Hsiao, C.-H., Yeh, S.-H., Wang, W.-K., chen, P.-J., Wang, J.-T., *et al.* (2003) Microbiologic characteristics, serologic responses, and clinical manifestations in severe acute respiratory syndrome, Taiwan. *Emerg Infec Dis* **9:** 1163–1167.

Hughes, T., Strongin, B., Gao, F.P., Vijayvergiya, V., Busath, D.D., and Davis, R.C. (2004) AFM visualization of mobile Influenza A M2 molecules in planar bilayers. *Biophys J* **87:** 311–322.

Kopp-Marsaudon, S., Leclère, Ph., Dubourg, F., Lazzaroni, R., and Aimé, J.P. (2000) Quantitative measurement of the mechanical contribution to tapping-mode atomic force microscopy images of soft materials. *Langmuir* **16:** 8432–8437.

Ksiazek, T.G., Erdman, D., Goldsmith, C.S., Zaki, S.R., Peret, T., Emery, S., *et al.* (2003) A novel coronavirus associated with severe acute respiratory syndrom. *N Engl J Med* **348:** 1953–1966.

Kuznetsov, Y.G., Datta, S., Kothari, N.H., Greenwood, A., Fan, H., and McPherson, A. (2002) Atomic force microscopy investigation of fibroblasts infected with wild-type and mutant murine leukemia virus (MuLV). *Biophys J* **83:** 3665–3674.

Kuznetsov, Y.G., Fan, A.L.H., and McPherson, A. (2004) Atomic force microscopy investigation of wild-type Moloney murine leukemia virus particles and virus particles lacking the envelope protein. *Virology* **323:** 189–196.

Kuznetsov, Y.G., Gurnonb, J.R., Ettenb, J.L.V., and McPherson, A. (2005) Atomic force microscopy investigation of a chlorella virus, PBCV-1. *J Struct Biol* **149:** 256–263.

Liu, G.Y., and Salmeron, M.B. (1994) Reversible displacement of chemisorbed n-alkanethiol molecules on Au (111)

surface: an atomic force microscopy study. *Langmuir* **10:** 367–370.

Magonov, S.N., Elings, V., and Papkov, V.W. (1997) AFM study of thermotropic structural transitions in poly (diethylsiloxane). *Polymer* **38:** 297–307.

Malkin, A.J., McPherson, A., and Gershon, P.D. (2003) Structure of intracellular mature vaccinia virus visualized by *in situ* atomic force microscopy. *J Virol* **77:** 6332–6340.

Marra, M.A., Jones, S.J.M., Astell, C.R., Holt, R.A., Brooks-Wilson, A., Butterfield, Y.S.N., *et al.* (2003) The genome sequence of the SARS-associated coronavirus. *Science* **300:** 1399–1404.

Miura, K., and Shukuya, Y. (1993) Comparison between atomic force microscopic images of ionic crystal surfaces in air and in dry argon. *Jpn J Appl Phys* **32:** 4752–4753.

Negishi, A., Chen, J., McCarty, D.M., Samulski, R.M., Liu, J., and Superfine, R. (2004) Analysis of the interaction between adeno-associated virus and heparan sulfate using atomic force microscopy. *Glycobiology* **14:** 969–977.

Nettikadan, S.R., Johnson, J.C., Mosher, C., and Henderson, E. (2003) Virus particle detection by solid phase immunocapture and atomic force microscopy. *Biochem Biophys Res Commun* **311:** 540–545.

Peiris, J.S.M., Lai, S.T., Poon, L.L.M., Guan, Y., Yam, L.Y.C., Lim, W., *et al.* (2003) Coronavirus as a possible cause of severe acute respiratory syndrome. *Lancet* **361:** 1319–1325.

Rota, P.A., Oberste, M.S., Monroe, S.S., Nix, W.A., Campagnoli, R., Icenogle, J.P., *et al.* (2003) Characterization of a novel coronavirus associated with severe acute respiratory syndrome. *Science* **300:** 1394–1399.

Xu, S., Laibinis, P.E., and Liu, G.Y. (1998) Accelerating the kinetics of thiol self-assembly on golds-A spatial confinement effect. *J Am Chem Soc* **120:** 9356–9361.

Yeh, S.-H., Wang, H.-Y., Tsai, C.-Y., Kao, C.-L., Yang, J.-Y., Liu, H.-W., *et al.* (2004) Characterization of severe acute respiratory syndrome coronavirus genomes in Taiwan: molecular epidemiology and genome evolution. *PNAS* **101:** 2542–2547.